RESEARCH ARTICLE

Dehydration of Methanol to Dimethyl Ether using Y Zeolite Nano-catalyst Prepared via Hydrothermal Technique

Hamid Ghaffari[1], Mohamad Mahdi Zerafat[2,*], Sahar Foorginezhad[1]

[1]Shiraz university, faculty of advanced technologies.

[2]Faculty of Advanced Technologies, Nano Chemical Engineering Department, Shiraz University, Shiraz, Iran.

ARTICLE INFO

Article History:
Received 2021-03-10
Accepted 2022-11-12
Published 2022-03-01

Keywords:
Y Nano-zeolite
Hydrothermal Synthesis
Template Free
Methanol conversion
Dimethyl ether

ABSTRACT

Y-type zeolite can be considered as one of the most applied zeolites at industrial scale, especially for catalytic transformations among various zeolites. Various synthesis techniques are employed to produce zeolite Y among which hydrothermal technique is considered as the most prevalent. In this study, synthesis of Y-type nano-zeolite was investigated through template-free hydrothermal technique. At various temperatures and aging times, zeolite Y was synthesized in the 10-30 nm size range with the first stage temperature of 25 °C and 87 °C as the second stage temperature. The as-synthesized zeolite was characterized using X-ray diffraction (XRD), Fourier-Transform Infrared (FTIR) spectroscopy, Field-Emission scanning electron microscopy (FE-SEM), Nitrogen adsorption–desorption, Transmission electron microscopy (TEM), and NH_3-TPD and utilized as the nano-catalyst in methanol to dimethyl ether (DME) conversion process. Based on the results, at 400 °C, 53.7 % conversion to DME was obtained with 100% purity using the hydrogen form of zeolite Y (H-Y) nano-catalyst. Natural zeolite is also considered as a proper additive to economize the product.

How to cite this article
Ghaffari H., Zerafat M. M., Foorginezhad S. Dehydration of Methanol to Dimethyl Ether using Y Zeolite Nano-catalyst Prepared via Hydrothermal Technique. J. Nanoanalysis., 2022; 9(1): 24-37. DOI: 10.22034/jna.2022.1925780.1249.

INTRODUCTION

Zeolites, either natural or synthetic, are crystalline or amorphous aluminosilicates with various applications in industry, including adsorption of materials such as nitrate and dyes [1], membrane separation [2, 3], solid desiccants for natural gas dehydration [4], catalysts [5], etc. Among various zeolites, Y-type zeolite can be considered as the most common at industrial scale especially in catalytic transformations [6]. The most important feature of zeolite is the mesoporous cavities facilitating molecular penetration into the structure; thus considered as the main reason for high catalytic activity [7]. Zeolite Y, is categorized as a medium silica type with a Si/Al ratio < 2.5.

Various synthetic procedures are employed to produce zeolite Y. Sol-gel method was the first proposed technique for this purpose [8], although hydrothermal technique is considered as the most prevalent. Generally, hydrothermal technique along with post-dealumination used to adjust the Si/Al ratio, depending on the application and performance, is the most utilized synthetic procedure [9]. Since zeolite Y can be directly synthesized with a maximum Si/Al values of ~3, all catalytically relevant materials must be prepared by post-synthesis de-alumination. Although variable temperature programs are also devised to attain small crystals without any templates, structure directing agents or templates can be used for the synthesis of small nanocrystals [10].

According to previous studies, Zeolite Y can be synthesized in the >100 nm size range through hydrothermal technique [11], using different templates such as tetramethylammonium hydroxide (TMAH) to adjust the particle size distribution [12]. In order to reduce the Zeolite Y size distribution, several researchers have taken advantage of twin templates. For

* Corresponding Author Email: *mmzerafat@shirazu.ac.ir*

Table 1. The designed experiments used to investigate the effect of temperature and time.

Sample	Time (min)		Temperature (^{0}C)	
	Step 1	Step 2	Step 1	Step 2
NaY1	24	54	40	87
NaY2	12	60	50	87
NaY3	12	54	25	90
NaY4	12	48	25	100

Residence time= 25 min, WHSV=8

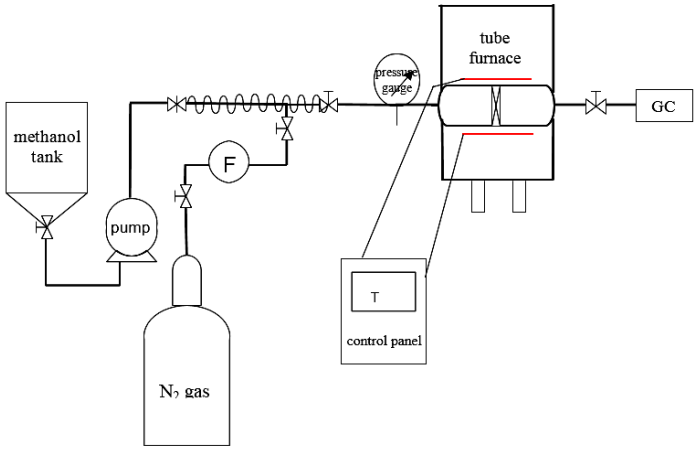

Fig. 1. Schematic of the equipment used for catalytic MTO conversion.

example, Holmberg et al. [13], used TMAH and tetramethylammonium bromide (TMAB) as main and co-templates, respectively. Moreover, concentration optimization for both templates led to the formation of zeolite particles in the 32-120 nm size range.

Template-free synthesis is another approach comprising of two heating stages, including nucleation and growth with or without template addition. Sang et al. [14], Synthesized Na-Y zeolite with small crystals using a two-stage variable temperature procedure without any organic templates, structure directing agents, seeding crystals, or other additives via hydrothermal technique. Initiation from low temperature leads to nucleation enhancement and higher temperature causes growth of the nuclei. The average particle size of the synthesized particles using the variable temperature program was 400 nm, while it was ~800 nm in terms of synthesis at constant temperature.

Due to the world oil reserve shortage and their ever-growing cost, universal demand for other raw resources such a natural gas or biomass is growing. Also, recent environmental concerns have escalated the inclination towards green technologies for production of gasoline. Also, it is expected that worldwide demand for polyolefins shows an increasing rate in near future. On the other hand, demand for ethylene and propylene commonly produced by cracking and fluid catalytic cracking of naphtha vapor is under a dramatic growth. Due to increasing demand for propene, specific production technique is highly required [15]. Production of both gasoline and light olefins is feasible through methanol conversion using acidic catalysts. This process is generally known as methanol to hydrocarbon (MTH) conversion which can be utilized to produce various hydrocarbons depending on the catalyst and processing conditions [16].

Among various MTH procedures, methanol to DME conversion is already practiced using catalysts such as γ-alumina [17], ZSM-5 [18], and many others. Production of other ethers is also practiced using various zeolites [19-21]. ZSM-5 has especially been considered as a promising

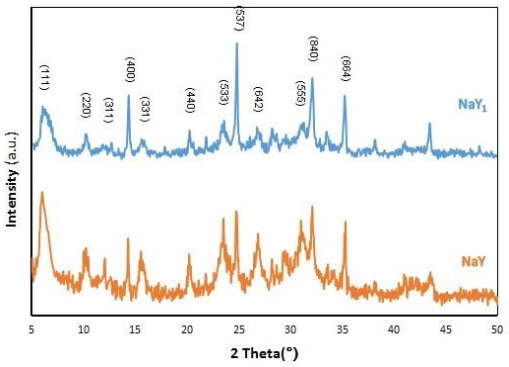

Fig. 2. XRD patterns of NaY and NaY_1 zeolite samples.

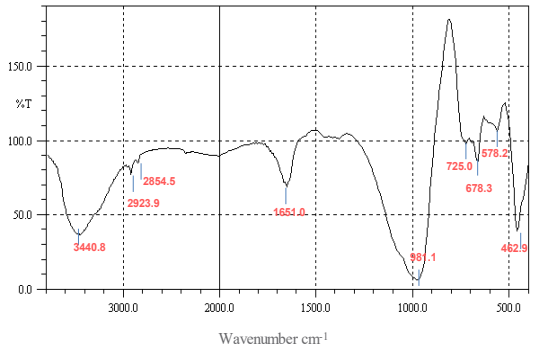

Fig. 3. FTIR spectrum of the as-synthesized NaY zeolite.

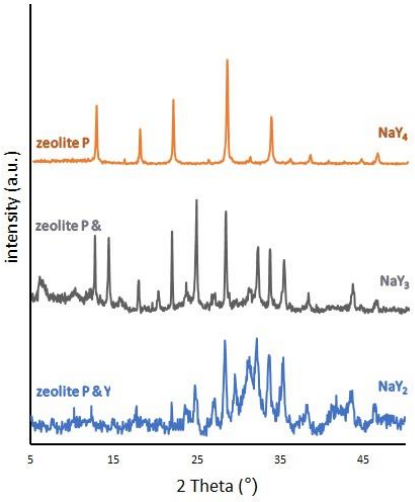

Fig. 4. XRD spectrum of zeolite samples NaY_2, NaY_3 and NaY_4.

candidate, but production of hydrocarbon as a byproduct and lack of total selectivity for the conversion of methanol to DME has provoked studies toward the investigation of other zeolite types like zeolite Y. For example, H-ZSM-5 exhibits a great performance in terms of catalytic activity and stability and despite the existence of strong acid sites, it is rather coke resistant due to shape selectivity; however, selectivity for DME is not 100%. Also, hydrocarbons are formed on the strong acid sites on the surface of the catalyst. In order to avoid coking and increasing the selectivity for DME, the strength of the acid sites must be reduced [18]. Besides, incorporating metal nanostructures inside catalyst pores [22] has been considered as a promising solution for the above mentioned problem. Moreover, the relationship between crystal size and performance of methanol to DME has been studied. According to previous studies, crystallite size reduction plays a vital role in catalyst effectiveness in terms of reducing the diffusion path [23]. Catizzone et al. [24] studied the effect of zeolite crystallite size on methanol-DME dehydration. Typically, zeolites were synthesized in the range of 0.1-10 μm and the catalytic performance was evaluated. According to the results, decreasing crystallite size down to 100 nm resulted in a reduction of inter-crystalline mass transfer limitation and acid sites accessibility enhancement. Consequently, the methanol apparent turnover frequency was improved while no by-product was detected for small particles. Also, decreasing the zeolite size down to 300-500 nm led to selectivity enhancement from 0.92 to 0.98. Furthermore, not only coke deposition diminished, but also catalyst regeneration performed at lower temperatures using nano-sized zeolites. Also, it was depicted in Masih et al. [25] that smaller crystallite size resulted in a high specific surface area followed by enhancement in catalytic lifetime.

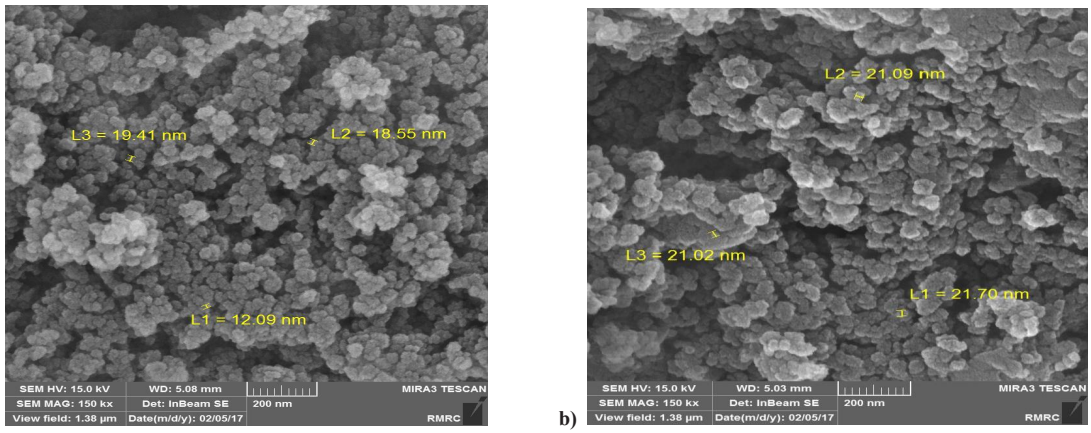

Fig. 5. FE-SEM images of samples (a) NaY and (b) NaY_1.

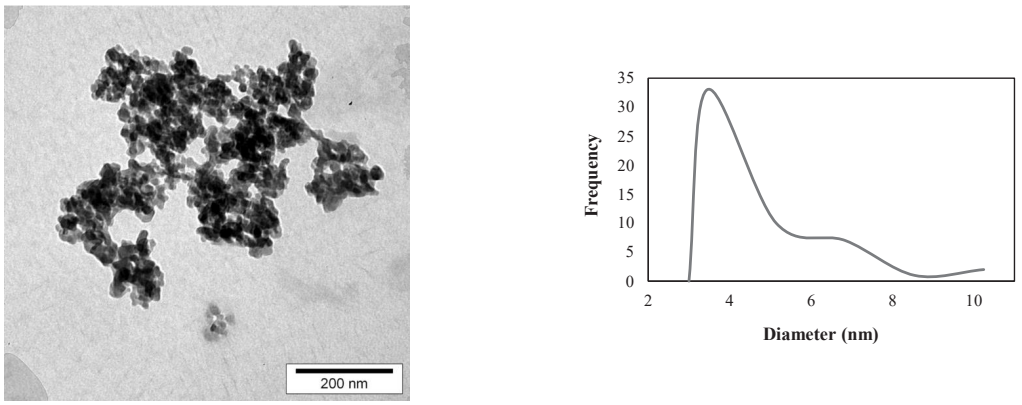

Fig. 6. (a) TEM images of zeolite NaY, and (b) PSD based on image analysis.

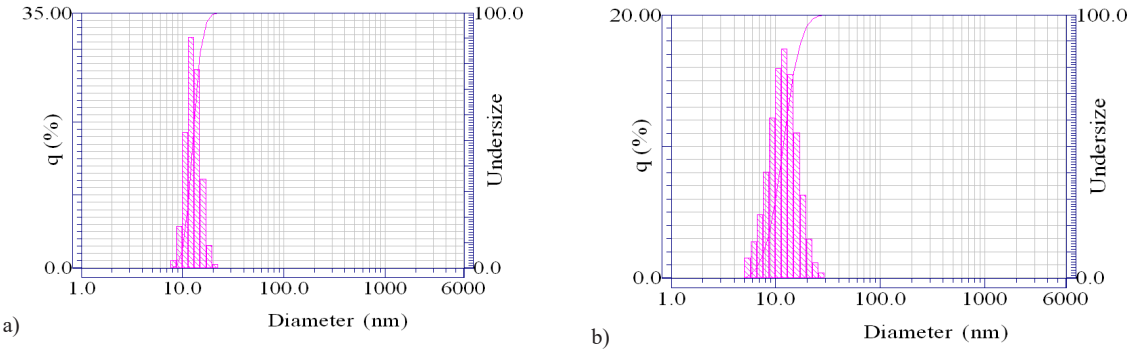

Fig. 7. Particle Size Analysis (PSA) of (a) NaY and (b) NaY_1 type zeolites.

Moreover, Cai et al. [26] demonstrated that the reaction rate was directly dependent on zeolite size and individual particles in the 60-100 nm range were more active compared to their agglomerated counterparts. In terms of DME synthesis from CO, higher DME production rates were obtained on smaller zeolite crystallites.

In this study, two stage synthesis of zeolite Y was performed, resulting in nanoscale Y zeolite. Due to the high rate of nucleation at low temperatures and growth of nuclei at high temperatures, synthesis time and temperature were monitored to reduce the particle size into the < 100 nm size range. Also, methanol conversion to DME was investigated using zeolite HY. Based on the literature review performed, zeolite Y has never been investigated

Table 2. BET analysis for NaY zeolite.

Specific Surface area (m^2/g)	229.1
Average mesopore diameter (°A)	70.3
Total pore volume (cm^3/g)	0.54
Micropore volume (cm^3/g)	0.07
Mesopore volume (cm^3/g)	0.47
V_{meso}/V_{total}	0.87

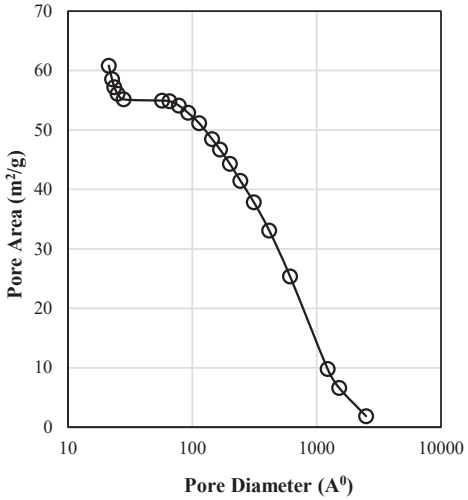

Fig. 8. The collective specific surface area based on pore diameters from BJH technique.

for DME production from methanol as a selective nano-catalyst. Based on the results, Y zeolite can be a great candidate for 100 % transformation of methanol to DME without the presence of other possible by-products.

EXPERIMENTAL INVESTIGATIONS

Materials and Methods

Materials

Colloidal silica ((LUDOX TMA, 34 wt. %) and aluminum isopropoxide (98 wt. %) were purchased from Sigma Aldrich. NaOH and ammonium hydroxide (25 %) were supplied by Merck Co. Natural Zeolite was also supplied by Semnan Region (Iran). Deionized water was used for preparation of all solutions. All reagents were of analytical grade and used as received without further purification.

Methods

Synthesis of zeolite Y nanocrystals

For the synthesis of zeolite NaY nanocrystals, a [Al_2O_3: SiO_2: Na_2O: H_2O] = [1:15.43:10:238] molar ratio was selected for the raw materials. First, solution A was prepared by mixing 1 g of aluminum isopropoxide with 5.5 ml of deionized water. Then, 2 g of NaOH was added to the mixture while magnetically stirred until the solution became clear. Solution B was also prepared by dissolution of 6.82 g of colloidal silica in 2.5 ml of distilled water. Solution B was slowly added to A in a Teflon liner. The autoclave was placed at 25-30 °C for 12 h and then placed in the oven at various temperatures for 54 h. Then, the content of the reactor was washed twice. The as-prepared powder was dried at the ambient temperature for 24 h and then at 90 °C for 1 h in the oven [27].

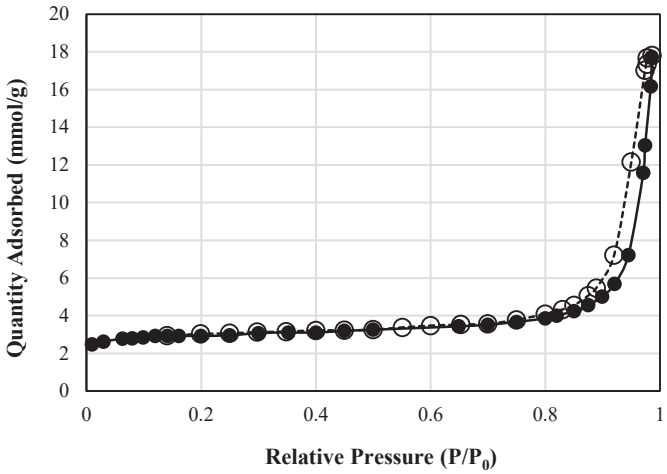

Fig. 9. Nitrogen adsorption-desorption curve for zeolite Y.

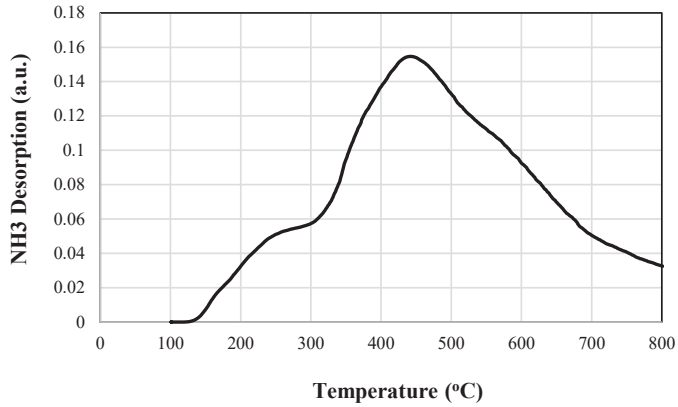

Fig. 10. The NH3-TPD spectra of Na-Y zeolite.

Synthesis of HY nanocrystals

Transformation of NaY zeolite to HY type is performed in this study as follows:

(1) 0.1 M ammonium hydroxide solution was prepared. Then 10 ml of the obtained solution was poured into the tubes containing 2 g of the as-prepared NaY zeolite.

(2) The suspension was magnetically stirred for 30 min to turn into slurry.

(3) The suspension is centrifuged to recover the solid content.

(4) The prepared solid was calcined in a furnace at 500 °C for 1 h to produce H-Y zeolite.

Methanol conversion reactor

The setup used for Methanol to Olefine (MTO) conversion consists of four main sections: **(1)** The tubular reactor, **(2)** Tubular furnace, **(3)** Nitrogen gas cylinder and, **(4)** Methanol reservoir and pump. A Schematic of the setup is given in Fig. 1.

Evaluation of the catalyst performance in the MTO conversion process is performed by controlling the methanol inflow into the reactor using a needle valve. The range of methanol flow for catalyst weight (WHSV) is adjusted at 5-25 [28]. Then, nitrogen gas is flown into the reactor at a rate of 20-50 ml/min. The catalyst is placed inside the furnace and the mixture of gases enters the reactor. Based on the residence time, the outflow valve is opened and the exit gases are sent for GC-Mass analysis. Methanol consumption (MC) is also calculated as follows from which methanol conversion can be obtained:

$$\mathrm{MC\ (g)} = \mathrm{Q_{N_2}} \times \frac{\mathrm{y_{DME}}}{\mathrm{y_{N_2}}} \times \mathrm{t} \times \rho_{\mathrm{DME}} \times \frac{1}{\mathrm{Mw_{DME}}} \times \frac{2\ \mathrm{mol\ MeOH}}{1\ \mathrm{mol\ DME}} \times \mathrm{Mw_{MeOH}} \quad (1)$$

$$\mathrm{Methanol\ Conversion\ (\%)} = \frac{\mathrm{g\ MeOH}}{\mathrm{Q_{MeOH}} \times \rho_{\mathrm{MeOH}} \times t} \times 100 \quad (2)$$

Where, Q is the flowrate, y molar fraction, t time and ρ the density.

Table 3. The results of the product at 400 °C and after 10, 25 and 50 minutes.

Constituents	10 min		25 min		50 min	
	Area under Peak (cm^2)	Composition (%)	Area under Peak (cm^2)	Composition (%)	Area under Peak (cm^2)	Composition (%)
N_2	3724993	56	4258523	60.5	4226676	61
DME	2954836	44	2771095	39.5	2662691	39

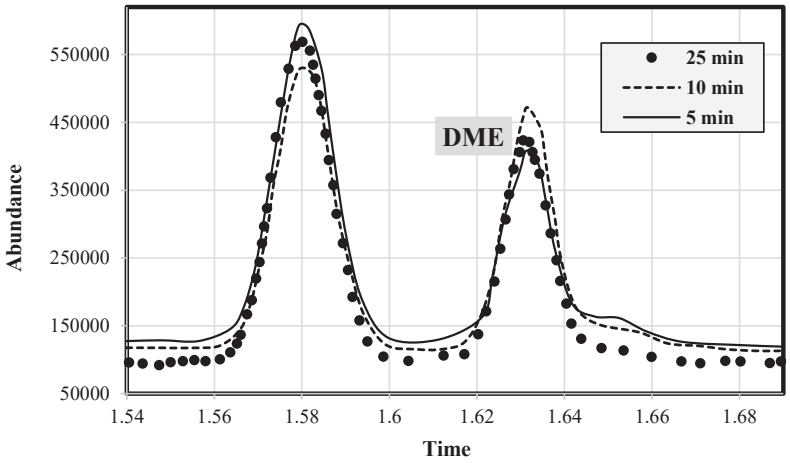

Fig. 11. The chromatogram of the product for methanol to DME process at 400 °C after 10, 25 and 50 min.

Design of Experiments

Various samples were synthesized as NaY, NaY_1, NaY_2, NaY_3, and NaY_4 at a constant molar ratio in order to investigate the effect of temperature and duration of steps. Table 1 shows a summary of the designed experiments.

Two zeolite types HY and NaY are investigated for methanol conversion in the designed tubular reactor. Also, variation of parameters is considered to analyze their effect on the performance of zeolite catalysts. Reactor temperature is varied in the 350-400 °C range with 50 °C steps. It is illustrated that, temperatures <350 lead to the reduction of catalyst performance, while higher temperatures are uneconomical [29]. The acidity of catalyst is also an effective parameter and it is reported that HY exhibits higher acidity in comparison with NaY which is evaluated at the optimal temperature. Acidity of zeolite-Y is performed using NH_3-TPD test which will be reported in the characterization section. The residence time is also considered as 25 and 50 min for NaY and HY, respectively. Weight hourly space velocity (WHSV) is equal to 8 in all experiments.

Characterization

Cumulative and density distribution of zeolite was evaluated and measured by Particle size Distribution (PSD) using Dynamic light scattering (DLS) particle size analyzer (JAPA Horiba LB550). XRD patterns of the produced zeolites are recorded by a Bruker AXSD8 using nickel-filtered Cu KαX-ray radiation at 40 kV and 40 mA and a scan rate of 3 degrees/min in the 2θ=5°-50° range. FT-IR spectrum (SHIMADZU 8300) was performed to verify chemical bonds of the as-synthesized particles. To analyze the particle size, FE-SEM was performed on a MIRA3TESCAN-XMU with a 30 kV acceleration voltage and also TEM images on a Philips CM 300 at 200 kV. To calculate the specific surface area and size of zeolite pores, Micromeritics ASAP2020 porosimetry device and Brunauer–Emmett–Teller (BET) theory were implemented. For the removal of trapped gas and water in zeolite cavities, degasification under vacuum was carried out at 150 ° C for 3 h. NH3-Temperature Programmed Desorption (NH3-TPD) experiments were carried out using a NanoSORD NS91 (made by Sensiran Co., Iran) apparatus. Si/Al ratio of

Table 4. The results of the product at 350 °C after 25 and 50 min.

Constituents	Area under Peak (cm^2)	Composition (%)
N_2	4252206	80
DME	1074602	20

Table 5. The results of the product at 400 °C after 50 min for HY zeolite.

Constituents	Area under Peak (cm^2)	Composition (%)
N_2	3218800	48
DME	3503028	52

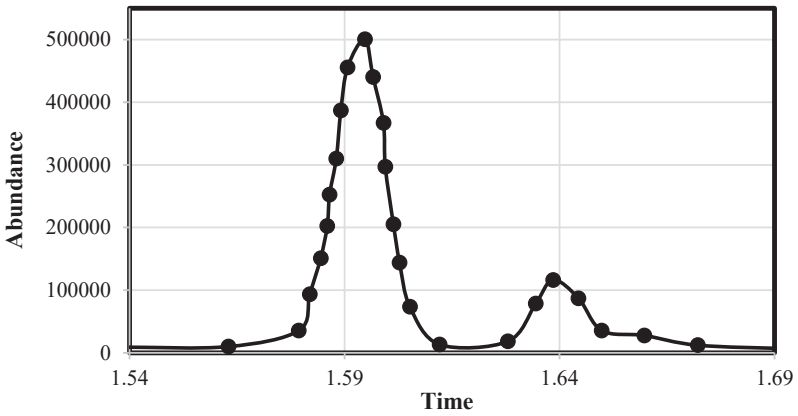

Fig. 12. The chromatogram of the product at 350 °C after 25 and 50 min.

synthesized zeolite was evaluated using Inductivity Coupled Plasma-Mass Spectrometry (ELAN 6100 DRC-e, Perkin Elmer).

RESULTS AND DISCUSSION

Crystallinity and Composition

The average yield of zeolite Y synthesized in this study was ~ 2 g for all samples, which is 11 wt.% of the raw materials [30]. The XRD patterns of NaY and NaY_1 zeolite samples are depicted in Fig. 2. According to XRD graphs, crystallinity of each sample was calculated using Origin Pro software and results illustrated that NaY crystallinity is ~ 50.3%, while NaY_1 consists of 64% crystalline content. Also, it can be inferred that, by increasing the temperature and duration of the first heating step, crystallinity is enhanced but the synthesized zeolite phase does not change with a small enhancement of temperature and step duration.

Fig. 3 shows FTIR pattern of the synthesized NaY zeolite. According to Fig. 3, the wavelengths of 462.9, 578.2, 678.3, 725 and 981.2 cm^{-1} are related to the Si-O or Al-O vibrations, double 4 rings, double 6 rings, O-Si-O, and T-O-T (T= Si or Al) bond, respectively, which confirms the formation of the relevant zeolitic network [31, 32].

Effect of temperature and time

Based on the XRD spectra of NaY_2, NaY_3, and NaY_4 (Fig. 4), increasing the temperature or duration of the second step, initiates the zeolite phase transformation, which can be attributed to increasing the growth rate of the nuclei followed by irregularities in the formation of the zeolitic phase. At 100 °C, zeolite P (NaY_4) appears in addition to zeolite Y [33].

Morphology and Size

FE-SEM images of NaY and NaY_1 samples and TEM image of NaY are shown in Figs. 5 and

Table 6. The results of the product at 400 °C after 50 min without zeolite.

Constituents	Area under Peak (cm^2)	Composition (%)
N_2	4448373	100
DME	0	0

Table 7. The results of the product at 400 °C after 25 min without natural zeolite.

Constituents	Area under Peak (cm^2)	Composition (%)
N_2	3972251	24.5
DME	1265338	75.5

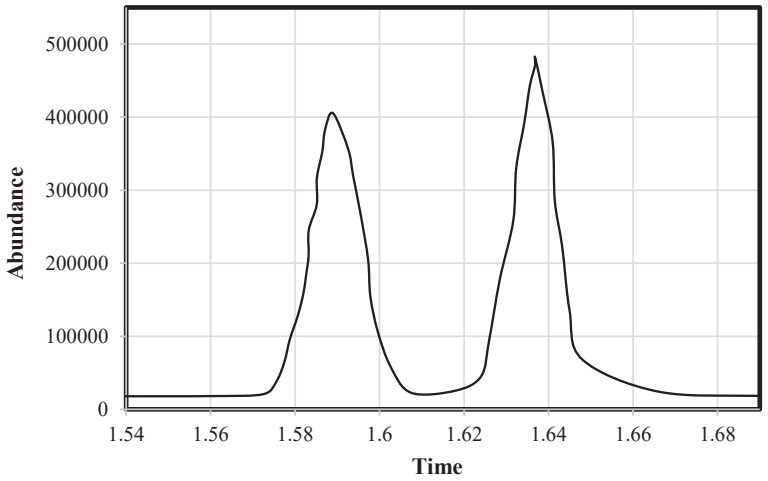

Fig. 13. The chromatogram of the product at 400 °C after 50 min for HY zeolite.

6, respectively. According to Figs 5 and 6, the size of NaY and NaY_1 particles varies in the ranges of 10-30 and 15-70 nm. Fig. 6 (b) depicts the particle size distribution of the synthesized zeolite based on image analysis of TEM micrograph. NaY_1 particle size enhancement can be attributed to the temperature rise and increasing the duration of the first heating step followed by decreasing the nucleation rate.

Zeolite NaY and NaY_1 particle sizes are given in Figs.7 (a) and (b) as cumulative and density distrisbution. According to the data, zeolites represent a uni-modal population distribution in the ranges of 9-22.5 and 6-30 nm with a 13 and 12.5 nm mean values, respectively

Specific surface area

Table 2 shows the results of BET analysis of NaY zeolite. The specific surface area is 229.1 (m^2/g) which can be related to the reduction of crystallinity and formation of amorphous phase [34]. It is conspicuous that, the average diameter of the cavities is 7.03 nm which is due to the formation of closed packing of zeolite nanoparticles upon drying. The high volume of the mesoporous cavities (87 %) not only is completely suitable for active catalytic materials such as noble metals, but also facilitates the entry of heavy molecules [35]. Based on Figs. 4 and 5, size distribution of NaY and NaY_1 zeolite falls in size ranges of 10-50 and 15-70 nm, respectively.

Also, Fig. 8 delineates the Barrett, Joyner, and Halenda (BJH) pore size distribution based on collective specific surface area. This method is suitable for mesopores and does not report the pores smaller than 1 nm. According to Fig. 8, the

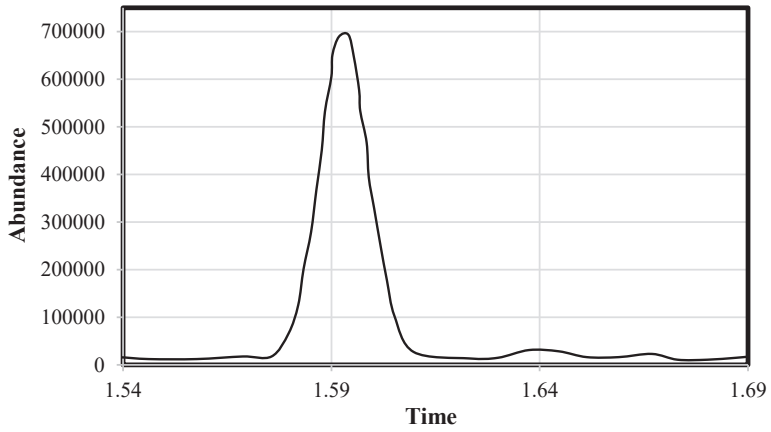

Fig. 14. The chromatogram of the product at 400 °C after 50 min without zeolite.

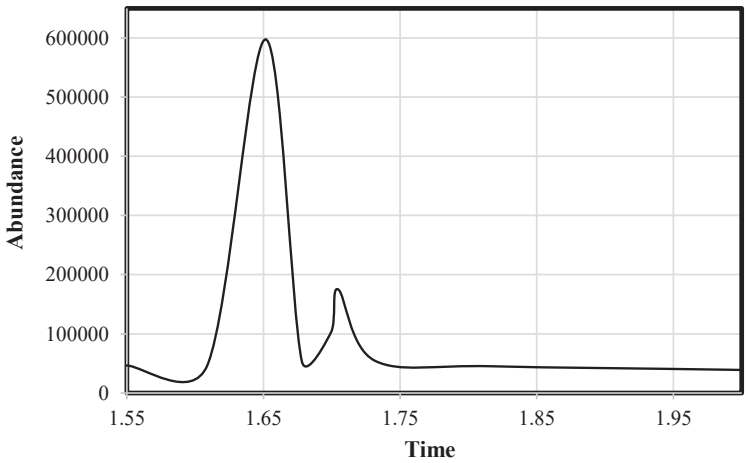

Fig. 15. The chromatogram of the product at 400 °C after 25 min without natural zeolite.

collective specific surface area reaches a constant value in the 50-100 nm range, which approves the absence of smaller pores. An increase in collective specific surface area at 2.4 nm shows the existence of pores in the micrometer range. This shows that the collective specific surface larger than 2 nm is almost similar to the external surface area by BET which approves 70 % of the pores as micro-porosity.

The hysteresis for the synthesized zeolite Y is given in Fig. 9 illustrates a mixture of type I and IV adsorption isotherms [36]. Precisely, gas hysteresis starts at a high P/P_0 in this isotherm type. On the other hand, fast desorption in early stage of pressure reduction and no further desorption depicts a high content of micro-porosities. Moreover, fast desorption in early stage can define the presence of large mesopores which readily desorb gas.

NH3-TPD acidity test

Fig. 10 represents the acidity of Na-Y zeolite evaluated by ammonia temperature-programmed desorption (NH3-TPD). The temperature at which ammonia desorption took place indicates the acid strength of the catalytic sites with the sites desorbing at a lower temperature being weaker. Na-Y Zeolite desorbed most of the ammonia at a temperature of 450 °C, which is associated to weak (or moderate) ammonia adsorption (h-peak). The presence of a shoulder in the curve at a temperature of 250 ^{0}C is also noteworthy, being associated to the stronger adsorption of NH_3 (l-peak) [37].

Gas Chromatography, Mass Spectrometry

Methanol to DME conversion is performed through methanol dehydration using an acidic catalyst. Due to the presence of Louis acid sites in

Table 8. The results of the product at 400 °C after 25 min with natural zeolite.

Constituents	Area under Peak (cm^2)	Composition (%)
N_2	1764247	43.5
DME	2290718	56.5

Table 9. A summary of results for methanol to DME conversion using various catalysts.

Catalyst	Temperature (°C)	Residence Time (min)	WHSVh^{-1}	Methanol flowrate (ml/min)	Conversion	main product	main product composition*
	350	25	8		17.7		
		50			17.7		
NaY Zeolite		10		0.15	39	DME	100
	400	25	8		32.3		
		50			31.7		
HY Zeolite	400	50	8	0.15	53.7	DME	100
Without natural zeolite	400	25	10	0.2	24.1	DME	100
Natural zeolite	400	25	10	0.2	19.3	DME	100
Without catalyst	400	25	10	0.2	0	--	--

* Percent DME produced relative to other products in the gas phase.

zeolite pores which lead to low reaction progress, zeolite Y should be modified [38]. Chromatogram results of NaY zeolite at 400 °C and after 10, 25 and 50 min of reaction are given in Table 3 and the corresponding chromatogram is also given in Fig. 11. Nitrogen and DME are also identified at 1.59 min and 1.64 min, respectively.

At 400 °C, conversion is very low and thus the zeolite catalyst entails modification. Various mechanisms are proposed for methanol to DME conversion. Based on Eq. 3, the presence of a proton (Bronstd acid site) or electron (Louis acid site) is essential for the production of methyl carbocation and reaction progress [38]:

$$CH_3OH + H^+ \leftrightarrow CH_3OH_2^+ \leftrightarrow CH_3^+ + H_2O$$
$$CH_3^+ + CH_3OH \leftrightarrow CH_3OCH_3 + H^+ \quad (3)$$

Another proposed mechanism is the in-situ formation of an oxonium ion, where zeolite Y converts the hydroxyl group by protonation into a group which leaves more readily; thus, ether is formed by nucleophilic attack of alcohol to the oxonium ion in a S_N2 type reaction [20].

Results for NaY zeolite at 350 °C and after 25 and 50 min are given in Table 4 and the chromatogram is also shown in Fig. 12.

At lower temperatures low activation energy results in a small conversion progress. Due to further reduction of activation energy, mixed zeolites like a mixture of ZSM-5 and zeolite Y presented better results. Table 5 represents the results of HY zeolite at 400 °C and after 50 min and related chromatogram is also shown in Fig. 13. Based on the results, conversion improvement can be related to the enhancement of acidic sites in the zeolite structure.

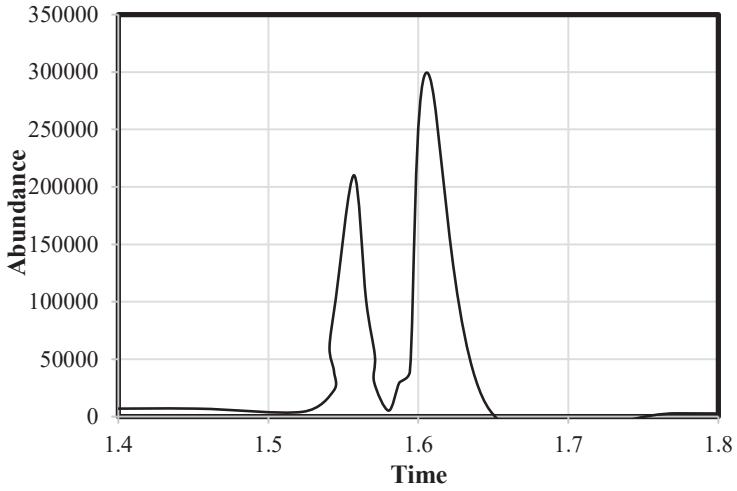

Fig. 16. The chromatogram of the product at 400 °C after 25 min with natural zeolite.

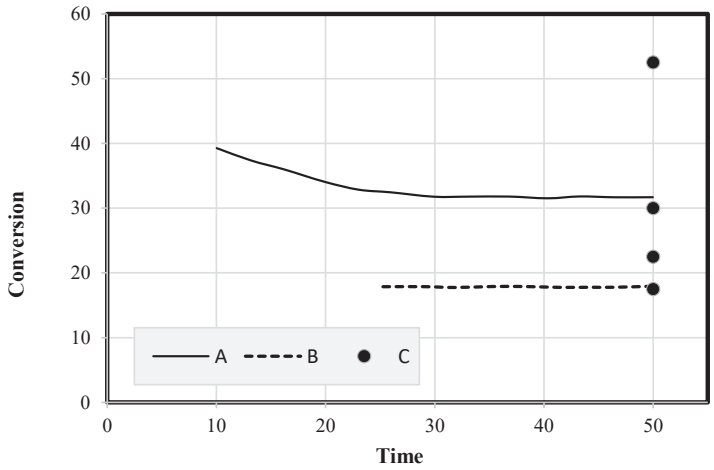

Fig. 17. The variety of conversion (a) NaY at 400 °C, (b) NaY at 350 °C and (c) Various catalysts at 400 °C.

Table 6 gives the results of the reactions in the absence of the catalyst and the corresponding chromatogram at 400 °C after 50 min is also shown in Fig. 14. Based on the results, no conversion is observed which approves the necessity of the zeolite presence as the catalyst.

Table 7 gives the results in the absence of natural zeolite with NaY at 400 °C and after 25 min and the corresponding chromatogram is also given in Fig. 15. It is worth noticing that, methanol flowrate is 0.2 ml/min and Nitrogen flowrate is also 40 ml/min.

Table 8 depicts the results in the absence of synthetic zeolite at 400 °C and after 25 min and the corresponding chromatogram is also shown in Fig. 16. In this case, the methanol flowrate is 0.2 ml/min and nitrogen flowrate is also 8 ml/min. Based on the results, natural zeolite has a significant effect on conversion and its presence causes promising effect on the economic feasibility of the process.

Fig. 17 shows conversion values in various experiments performed in this study. According to the results, natural zeolite becomes inactive faster than the synthetic zeolite. Based on Fig. 17, the highest conversion is obtained at 400 °C for HY zeolite. This is in a good accordance with the enhancement of acidic sites in the zeolite structure previously elaborated. A summary of results is also given in Table 9.

CONCLUSIONS

In this study, template-free synthesis of NaY zeolite was carried out in the size range of 10-30 nm. The two-step synthesis technique involves

applying proper conditions in the first stage and the growth of the nuclei in the second one. This leads to the synthesis of nano-crystalline zeolite Y and controlling synthesis parameters such as temperature and step duration. XRD analysis shows that in both steps a small change in temperature and time, causes a variation of particle size, crystallinity, and the final transformation of the prevalent zeolite phase. With the synthesis of zeolite particles at nanoscale, mesoporous cavities are produced proportional to their size upon drying. According to BET analysis, this constitutes 87% of the total pore volume, which makes it a great candidate for catalytic applications. Future work can be focused on investigating the effect of size on the efficiency of the process and also addition of various functionalities to zeolite such as metal oxides for further improvement in DME production amount.

CONFLICT OF INTEREST

The authors declare no conflict of interest.

NOMENCLATURE

XRD	X-ray diffraction
FTIR	Fourier-Transform Infrared Spectroscopy
FE - SEM	Field-Emission scanning electron microscopy
TEM	Transmission electron microscopy
TPD	Temperature-programmed desorption
MTH	Methanol to Hydrocarbon
MTO	Methanol to Olefin
WHSV	Methanol flow to catalyst weight
PSD	Particle size distribution
DLS	Dynamic light scattering
BET	Brunauer–Emmett–Teller
BJH	Barrett, Joyner, and Halenda
DME	Dimethyl ether

REFERENCES

1 Meftah T., Zerafat M. M., (2016), Nitrate Removal from Drinking Water using Organo-silane Modified Natural Nano-zeolite. Int. J. Nanosci. Nanotech. 12: 223-232.

2 Ghaee A., Zerafat M. M., Askari P., Sabbaghi S., Sadatnia B., (2017), Fabrication of Polyamide Thin Film Nanocomposite Membranes with Enhanced Negative Charge for Nitrate Removal. J. Environ. Tech. 38: 772-781. https://doi.org/10.1080/09593330.2016.1231223

3 Foorginezhad S., Zerafat M.M., (2017), Microfiltration of Cationic Dyes using Nano-clay Membranes. Ceramics Int. 43: 15146-15159. https://doi.org/10.1016/j.ceramint.2017.08.045

4 Gandhidasan P., Al-Farayedhi A. A., Al-Mubarak A.A., (2001), Dehydration of natural gas using solid desiccants. Energy. 26: 855-868. https://doi.org/10.1016/S0360-5442(01)00034-2

5 Pebriana R., Mujahidin D., Syah Y. M., (2017), The zeolite mediated isomerization of allyl phenyl ether. Mater. Res. Express. 4: 044004. https://doi.org/10.1088/2053-1591/aa6ac5

6 Zhao J., Wang G., Qin L., Li H., Chen Y., Liu B., (2016), Synthesis and catalytic cracking performance of mesoporous zeolite Y. Catalysis Commun. 73: 98-102. https://doi.org/10.1016/j.catcom.2015.10.020

7 Lutz W., (2014), Zeolite Y: Synthesis, Modification, and Properties-A Case Revisited. Advances Mater. Sci. Eng. 1-20. https://doi.org/10.1155/2014/724248

8 Barrer R., Meier W., (1958), Structural and ion sieve properties of a synthetic crystalline exchanger, Transact. Faraday Society. 54: 1074-1085. https://doi.org/10.1039/tf9585401074

9 Salman N., Ruscher C. H., Buhl J. Chr., Lutz W., Toufar H., Stocker M., (2006), Effect of Temperature and Time in the hydrothermal treatment of HY zeolite. Micropor. Mesopor. Mater. 90: 339-346. https://doi.org/10.1016/j.micromeso.2005.09.032

10 Holmberg B. A., Wang H., Norbeck J. M., Yan Y., (2003), Controlling size and yield of zeolite Y nanocrystals using tetramethylammonium bromide. Micropor. Mesopor. Mater. 59: 13-28. https://doi.org/10.1016/S1387-1811(03)00271-3

11 Berger C., Gläser R., Rakoczy R. A., Weitkamp J., (2005), The synthesis of large crystals of zeolite Y re-visited. Micropor. Mesopor. Mater. 83: 333-344. https://doi.org/10.1016/j.micromeso.2005.04.009

12 Shen Y., Manning M. P., Warzywoda J., Sacco A., (2002), Synthesis of Zeolite Y Nanocrystals from Clear Solutions. MRS Proceedings, 740. https://doi.org/10.1557/PROC-740-I7.16

13 Holmberg B. A., Wang H., Yan Y., (2004), High silica zeolite Y nanocrystals by dealumination and direct synthesis. Micropor. Mesopor. Mater. 74: 189-198. https://doi.org/10.1016/j.micromeso.2004.06.018

14 Sang S., Liu Z., Tian P., Liu Z., Qu L., Zhang Y., (2006), Synthesis of small crystals zeolite NaY. Materials Letters. 60: 1131-1133. https://doi.org/10.1016/j.matlet.2005.10.110

15 S. Kvisle, T. Fuglerud, S. Kolboe, U. Olsbye, K. P. Lillerud, and B. V. Vora, "Methanol-to-Hydrocarbons," in Handbook of Heterogeneous Catalysis, ed: Wiley-VCH Verlag GmbH & Co. KGaA, 2008. https://doi.org/10.1002/9783527610044.hetcat0149

16 M.W. Erichsen, "The methanol-to-hydrocarbons reaction : Influence of acid strength on the mechanism of olefin formation," ed, 2010.

17 F. Faoof, M. Taghizadeh, A. Eliassi, F. Yaripour, Effects of temperature and feed composition on catalytic dehydration of methanol to dimethyl ether over γ-alumina, Fuel 87 (2008) 2967-2971. https://doi.org/10.1016/j.fuel.2008.03.025

18 Y. Fu, T. Hong, J. Chen, A. Auroux, J. Shen, Surface Acidity and dehydration of methanol to dimethyl ether, Thermochimica Acta 434 (2005) 22-26. https://doi.org/10.1016/j.tca.2004.12.023

19 Z. Mobaraki, H. Moghanian, Kh. Faghihi, M. Shabanian, Novel Semi-Crystalline, Soluble and Magnetic Poly(imideether)/Zeolite Nanocomposites: Synthesis, Characterization and Computational Study, J. Inorganic & Organometallic Polymers & Materials 28 (2018) 1072-1089. https://doi.org/10.1007/s10904-018-0792-0

20 M.A. Bodaghifard, H. Moghanian, A. Mobinikhaledi, F. Esmaeilzadeh, Microwave-Assisted Efficient Synthesis of Azlactones Using Zeolite NaY as a Reusable Heterogeneous Catalyst, Inorganic & nano-metal chemistry 47 (2017) 845-849. https://doi.org/10.1080/15533174.2016.1212242
21 A. George, Z. Olah, T. Shamma, G.K. Surya Prakash, Dehydration of alcohols to ethers over Nafion-H, a solid perfluoroalkanesulfonic acid resin catalyst, Catalysis Letters 46 (1997) 1-4. https://doi.org/10.1023/A:1019069107667
22 J. Zheng, J. Ma, Y. Wang, Y. Bai, X. Zhang, R. Li, Synthesis and catalytic property of a zeolite composite for preparation of dimethyl ether from methanol dehydration, Catalyst Letters (2009) 130: 672-678. https://doi.org/10.1007/s10562-009-0012-1
23 V. Valtchev, L. Tosheva, Porous nanosized particles: preparation, properties, and applications. Chemical reviews, 113 (2013) 6734-6760. https://doi.org/10.1021/cr300439k
24 E. Catizzone, S. Van Daele, M. Bianco, A. Di Michele, A. Aloise, M. Migliori, G. Giordano, Catalytic application of ferrierite nanocrystals in vapour-phase dehydration of methanol to dimethyl ether, Applied Catalysis B: Environmental, 243 (2019) 273-282. https://doi.org/10.1016/j.apcatb.2018.10.060
25 D. Masih, S. Rohani, J.N. Kondo, T. Tatsumi, Low-temperature methanol dehydration to dimethyl ether over various small-pore zeolites, Applied Catalysis B: Environmental, 217 (2017) 247-255. https://doi.org/10.1016/j.apcatb.2017.05.089
26 M. Cai, A. Palčić, V. Subramanian, S. Moldovan, O. Ersen, V. Valtchev, A.Y. Khodakov, Direct dimethyl ether synthesis from syngas on copper-zeolite hybrid catalysts with a wide range of zeolite particle sizes, J. Catalysis, 338 (2016) 227-238. https://doi.org/10.1016/j.jcat.2016.02.025
27 H. Ghaffari, MSc Thesis (in Persian), Hydrothermal synthesis of Y zeolite and its application as nanocatalyst in methanol conversion process, Shiraz University, Shiraz, Iran (2017).
28 H.S. Mar, Catalytic conversion of methanol/dimethylether to light olefins over microporous Silicoaluminophosphates catalysts, Dissertation/Thesis, 2010.
29 C.K. Narula, B.H. Davison, and M. Keller, "Catalytic conversion of alcohols to hydrocarbons with low benzene content," ed: Google Patents, 2016.
30 Shen B., Qin Z., Gao X., Lin F., Wang B., Xu C., (2011), Mesoporous Y zeolite with homogeneous aluminum distribution obtained by sequential desilication-dealumination and its performance in the catalytic cracking of cumene and 1,3,5-triisopropylbenzene. J. Catalysis. 278: 266-275. https://doi.org/10.1016/j.jcat.2010.12.013
31 Bnmner G.O., Meier W. M., (1989), Framework density distribution of zeolite-type tetrahedral nets. Nature. 337: 146-147. https://doi.org/10.1038/337146a0
32 Davis M. E., Lobo R. F., (1992), Zeolite and molecular sieve synthesis. Chem. Mater. 4: 756-768. https://doi.org/10.1021/cm00022a005
33 Byrappa K., Yoshimura M., (2001), Hydrothermal Synthesis and Growth of Zeolites, Handbook of Hydrothermal Technology, ed Norwich, NY: William Andrew Publishing. 315-414. https://doi.org/10.1016/B978-081551445-9.50007-6
34 H. Awala, J.P. Gilson, R. Retoux, P. Boullay, J.M. Goupil, V. Valtchev, S. Mintova, Template-free nanosized faujasite-type zeolites, Nature Materials 14 (2015) 447-451. https://doi.org/10.1038/nmat4173
35 Zhao J., Wang G., Qin L., Li H., Chen Y., Liu B., (2016), Synthesis and catalytic cracking performance of mesoporous zeolite Y. Catalysis Commun. 73: 98-102. https://doi.org/10.1016/j.catcom.2015.10.020
36 J. Keller, R. Staudt, (2005), Gas adsoption equilibria, experimntal methods and adsorption isotherms, Chapter 7, 361-363.
37 A.W. Chester, E.G. Derouane, Zeolite Characterization and Catalysis, chapter 3, Determination of Acid/Base Properties by Temperature Programmed Desorption (TPD) and Adsorption Calorimetry (2009).
38 Agostinho L.C.L., Barbosa C., Nascimento L., Rodbari J., (2013) Catalytic dehydration of methanol to dimethyl ether (DME) using the Al62,2Cu25, 3Fe12,5 Quasicrystalline alloy," J. Chem. Eng. Process. Technol. 4: 2-8.